Increasing population exposure to future heatwaves influenced by land-atmosphere interactions

Jingwei Zhou (jingwei.zhou@wur.nl)
Wageningen University & Research https://orcid.org/0000-0003-0012-0929
Adriaan J. Teuling
Wageningen University & Research https://orcid.org/0000-0003-4302-2835
Sonia Seneviratne
Swiss Federal Institute of Technology in Zurich https://orcid.org/0000-0001-9528-2917
Annette Hirsch
The University of New South Wales

Article

Keywords:

Posted Date: August 29th, 2022

DOI: https://doi.org/10.21203/rs.3.rs-1990379/v1

Increasing population exposure to future heatwaves influenced by land-atmosphere interactions

Jingwei Zhou [1, 2]*, Adriaan J. Teuling [1], Sonia I. Seneviratne [3], Annette. L. Hirsch [4,5]*

[1]Hydrology and Quantitative Water Management Group, Wageningen University & Research, Wageningen, Netherlands

[2]Research School of Earth Sciences, The Australian National University, Canberra, Australia

[3]Institute for Atmospheric and Climate Science, ETH Zurich, Zürich, Switzerland

[4]ARC Centre of Excellence for Climate Extremes, The University of New South Wales, Sydney, Australia

[5]Climate Change Research Centre, The University of New South Wales, Sydney, Australia

*e-mail: jingwei.zhou@wur.nl; annette.l.hirsch@gmail.com

Abstract

Heatwaves have significant effects on ecosystems and human populations. Human habitability is impacted severely as human exposure to heatwaves is projected to increase, in which land-atmosphere interactions make a vital contributing factor. Future risk of heatwaves is substantial and imminent worldwide. Increasing heatwave trends have demonstrated the need of effective measures for adaptation to persistent hot temperature extremes and ambitious mitigation to limit further increases in heatwave severity.

This study examines whether the projected intensification of land-atmosphere interactions contributes to projected increases in heatwave events and what this may mean for future population exposure to heatwaves. With the intensification of land-atmosphere interactions, heatwaves are found to increase by up to 40 days, intensify by up to 4.5 °C averagely in global land regions, with increasing frequency of 33% over most mid-latitude land regions by 2070–2100 under the RCP8.5 high emissions scenario. Furthermore, dry soil moisture conditions have a significant role in projected increases of multiple heatwave characteristics regionally compared with the global land area. Land-atmosphere interactions contribute as much as 35.7% to an average of 39.3% more of today's global population exposure to heatwaves. Our results highlight contributions from land-atmosphere interactions on both heatwaves and their impacts on human population.

Introduction

Recent years have seen an increasing trend in heatwave duration, frequency, and intensity worldwide[1-6]. For the Northern Hemisphere, the 2003 European heatwave and 2010 Russian heatwave were two high-impact events which have been studied extensively[7-11]. The five warmest summers for the Northern Hemisphere have occurred since 2015, while the 2020 summer (Jun. 2020–Aug. 2020) tops among the five, setting the record as an anomaly of 1.17 °C above the 20th-century average for such period[12]. In particular, in the 2020 North Hemisphere summer, the most notable warm temperature anomalies were present across the southwestern and northeastern US, eastern Canada, and northern Russia. Across these regions the seasonal temperature was at least 2.0°C above average[12]. In 2022, extreme heat events continued throughout India and Pakistan, where the temperature in Pakistan recorded its first 50°C of the year. For the Southern Hemisphere, Australia has also experienced an increasing trend in heatwaves since 1981 with higher intensity and longer duration[13-15]. The summer from Dec. 2019 to Feb. 2020 was the hottest on record for Australia. During December 2019, 11 days, in which the national area-averaged maximum was 40 °C or above, were among this unusually extended period of heatwave over much of Australia. In the context of global land, the year 2020 ranked the warmest year in the 141-year record and had an average land temperature anomaly of +1.59 °C[16].

The effect of land-atmosphere interactions in amplifying hot temperature extremes in past and present climate has been widely explored in recent decades[17-20]. Some previous heatwave-related studies had a regional focus[7,14,18,21,22]. However, research comparing the mechanisms of heatwaves across regions using a consistent methodology is more limited. As the spatial heterogeneity of land surface conditions (e.g., vegetation, soil moisture, and land use), precipitation variability, and atmospheric dynamics contributes to regional differences in land-atmosphere interactions and heatwaves[15,17,23], the

quantification and distinction of how much regional land surface contributions to heatwaves vary globally, is of primary importance. In particular, it is necessary to avoid generalising land surface contributions when it has been demonstrated that land-atmosphere interactions vary spatially[17]. Additionally, since the 1950s, there has been an increasing trend in heatwave duration, frequency, and intensity over many regions in the world[3,6,11,24-26]. As the impacts from heatwaves have increased in the recent past and are projected to increase under future warming[2,5,27,28], investigating future changes of land surface amplification of hot temperature extremes changes would significantly help to understand regional differences in projected heatwave characteristics.

Heatwaves tend to increase human morbidity and mortality[29-32]. Existing research is often focused on the population exposure to heatwaves per se and its influence on the mortality and morbidity of people[29,33]. Yang et al. (2021) found that heat-related excess mortality is projected to increase from 1.9% in the 2010s to 5.5% (0.5–9.9%) in the 2090s under RCP8.5 in China[34]. With different heatwave definitions used, heatwave-related mortality risks increased by a range of 3–16% globally[35]. However, population exposure to heatwaves is rarely correlated to drivers to heatwaves such as land-atmosphere interactions. Understanding land surface impacts on population exposure to heatwaves will benefit the development and improvement of future community adaption methods and mitigation policies against heatwave impacts. In this study we investigate the relative contributions of land-atmosphere interactions to increases of heatwave characteristics and how this relates to future changes in population exposure to extreme heat.

Results

We use the Global Land Atmosphere Coupling Experiment—Coupled Model Intercomparison Project phase 5 (GLACE—CMIP5)[19] to investigate the spatial evolution of land-atmosphere interactions and heatwave characteristics. The set-up of the GLACE-CMIP5 experiment is briefly described hereafter, for more details please refer to Seneviratne et al. (2013). GLACE—CMIP5 is based on simulations from six climate models (Tab. 1), which are, the Community Earth System Model (CESM), European Centre-Earth (EC-Earth), model of Geophysical Fluid Dynamics Laboratory (GFDL), model of Institut Pierre-Simon Laplace IPSL), Australian Community Climate and Earth System Simulator (ACCESS), and Max Planck Institute Earth System Model (MPI-ESM). Simulations from these models span the period 1950 to 2100 (more details can be found in GLACE-CMIP5 of Methods) and derived under a RCP8.5 high emissions scenario. To quantify the population exposure to heatwave characteristics, gridded data of global population count in 2020 was also included in this study, which comes from NASA SocioEconomic Data and Applications Center (SEDAC)[36]. All the population data and climate model data have been interpolated to a common grid with a resolution of 3.75° longitude by 2.5° latitude using a conservative remapping approach[37,38].

We use a modified excess heat factor (EHF) to define heatwaves. If at least three consecutive days where the daily mean temperature exceeds a calendar-day 90th percentile temperature threshold (T_{90}), which is calculated for a reference period (1950–2014), these days will be characterized as the heatwave days. For each climate model within the GLACE—CMIP5, a specific T_{90} throughout the present period of 1980–2010 and future period of 2070–2100 is adopted in this study. Five heatwave characteristics are studied in this paper, including heatwave mean intensity (HWMt), heatwave peak intensity (HWAt), heatwave duration (HWD), heatwave frequency (HWF), and heatwave severity (more details can be

found in the heatwave identification and classification of the Methods).

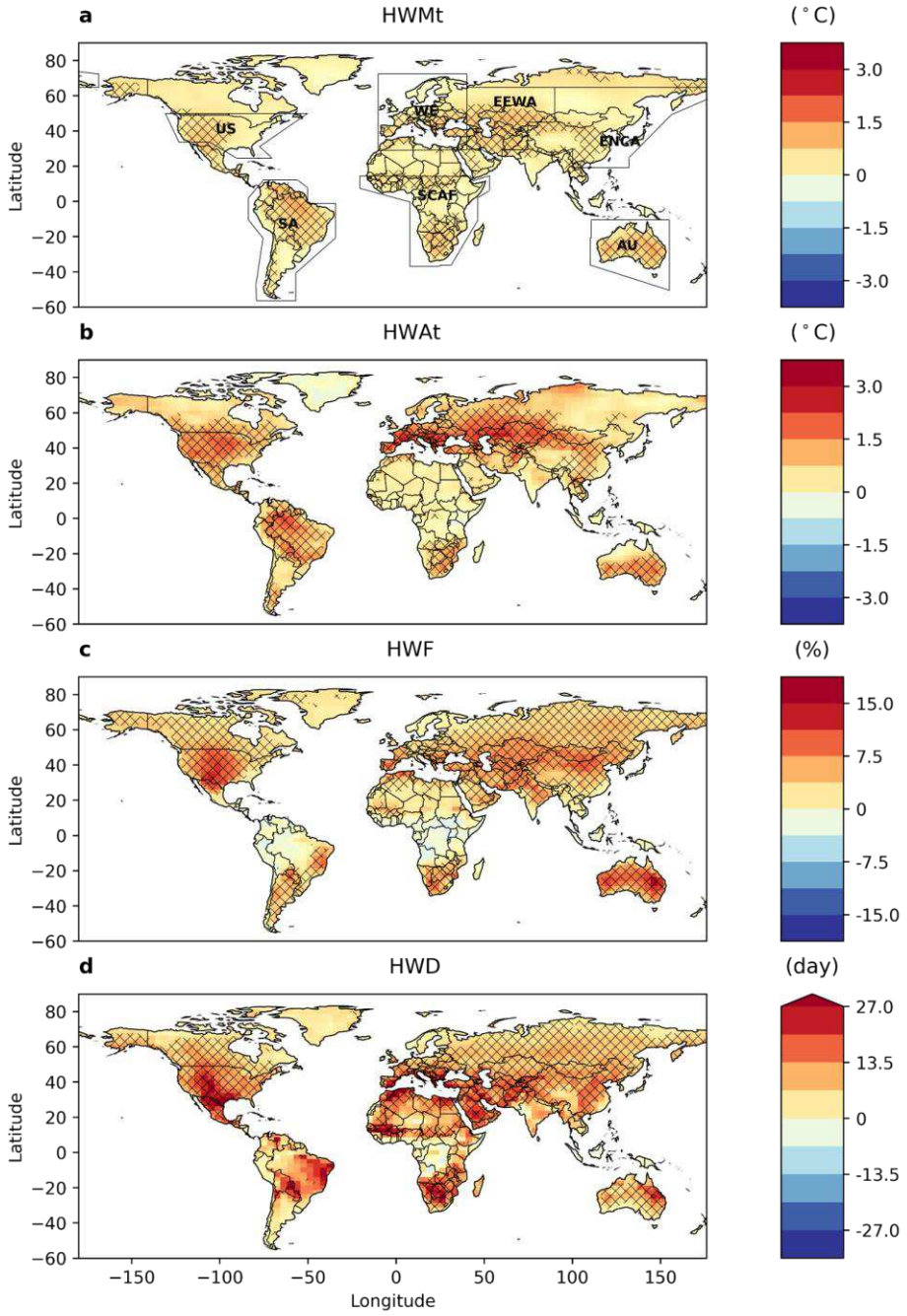

Fig. 1 | Spatial distributions of changes in land-atmosphere interactions in the forms of different heatwave characteristics. a–d, The influences of land-atmosphere interactions (indicated by the values of the four heatwave characteristics expressed in CTL−ExpA) on heatwave mean intensity (**a**; HWMt), peak intensity (**b**; HWAt), frequency (**c**; HWF), duration (**d**; HWD) are displayed across two 30-year periods. The change is between 1980–2010 (PRE) and 2070–2100 (FUT). Hatching indicates where the bias is significantly different at 99% confidence level based on Mann-Whitney rank tests. The analysis is limited to the summer-centering periods. The extensions in color bars indicate values beyond the limits. Oceans have been masked in white. Seven domains are set for this study: East, North, and central Asia (ENCA); Australia (AU); the US; West Europe (WE); East Europe and West Asia (EEWA); Southern and central (SCAF, African continent below the Sahara Desert) Africa; South America (SA).

Each of the six climate models within GLACE—CMIP5 performs a fully-coupled control run (CTL), and two experiments (ExpA and ExpB) where soil moisture is prescribed. In this paper, only one of the experiments (ExpA) is used with CTL to quantify land-atmosphere interactions in the form of CTL–ExpA[20]. Soil moisture in ExpA is prescribed by the 1971–2000 climatological values calculated from the control simulation. To understand the contribution of land-atmosphere interactions to each of the heatwave characteristics, estimates of each ensemble (CTL and ExpA) are compared (Figure 1). Fig. 1 illustrates that influences of land-atmosphere interactions are increasing over most land regions. One of the reasons for the intensification is that the difference of soil moisture between CTL and ExpA is becoming greater as the soil moisture evolves in CTL by the design of the experiment. Estimation of the difference in land-atmosphere interactions between future period (2070–2100) and present period (1980–2010) commonly reaches about 1.5 °C for heatwave mean intensity (Fig. 1a), 2.5 °C for peak intensity (Fig. 1b), 15% for frequency in some of the land regions (Fig. 1c), and about 20 days for their effects on duration in most of the land regions (Fig. 1d). Central Asia, Australia, South Africa, North of Africa, East of Brazil, most parts of the Europe, Mid-West of the USA, Mid-West of Canada tend to have significant intensification on all the four heatwave characteristics (HWMt, HWAt, HWF, and HWD) as a result of land-atmosphere interactions (Fig. 1).

The effects of land-atmosphere interactions are diverse in the forms of four heatwave characteristics (HWMt, HWAt, HWF, and HWD). For heatwave mean intensity and peak intensity, the difference between ExpA and CTL increases across West USA, Brazil, South Africa, West Asia, central Asia, and Australia, where the difference is already great in the period of 1980–2010 (Fig. S2a, c). For heatwave frequency and duration the large change of CTL–ExpA spreads over most of US and the Eurasia, and also throughout North Africa (Fig. 1c,d); additionally, the impact from the soil moisture is weakened for

heatwave frequency in central Africa and the northern parts of South America (Fig. 1c).

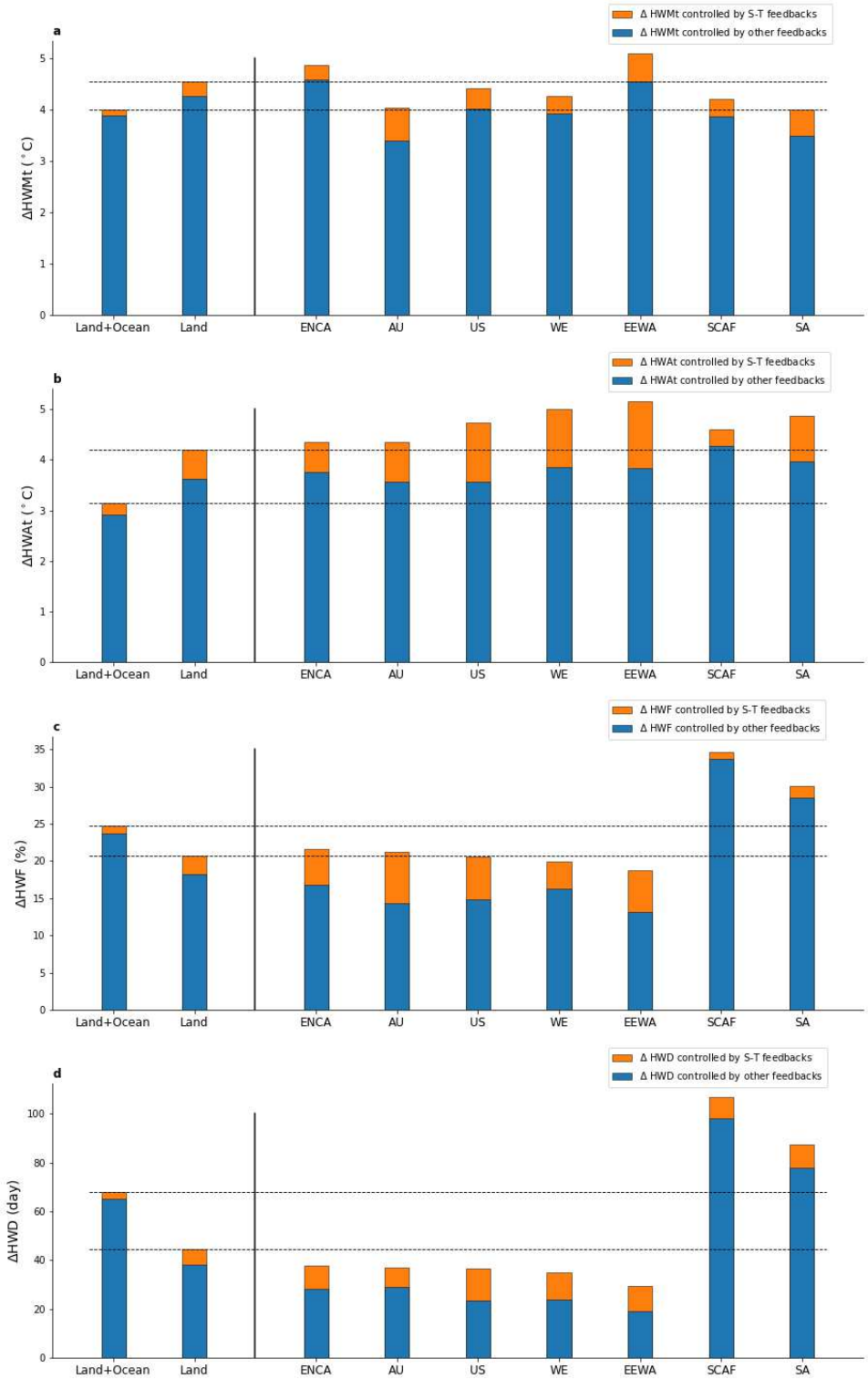

Fig. 2 | Projected change in global and regional heatwave characteristics. a–d, Increases of heatwave mean intensity (**a**; HWMt), peak intensity (**b**; HWAt), frequency (**c**; HWF), and duration (**d**; HWD) induced by land-atmosphere interactions and other factors are displayed across two 30-year periods. The change is between 2070–2100 and 1980–2010. The orange part indicates contribution of land-atmosphere interactions; the blue part

indicates other factors such as cloud cover, radiation, and precipitation. The domains are delineated in both Fig. 1 and Fig. 3, the oceans are excluded for these domains.

Heatwaves tend to be longer, more intense, and affecting more land regions by the end of the century when including the effects of land-atmosphere interactions (Figure 2). In the land regions globally, the average temperature of heatwaves (HWMt) is projected to increase by more than 4 °C in the future period (2070–2100) (Fig. 2a); the peak of heatwave temperatures (HWAt) is also projected to increase by more than 4 °C (Fig. 2b); more heatwaves are estimated to occur in the future, the increase of heatwave frequency reaches 20% (Fig. 2c); the increase of heatwave duration is substantial, which can be more than 40 days yearly (Fig. 2d). Among the four heatwave characteristics, the increases of heatwave frequency and duration are greater in all the globe (land and ocean) compared with those in just land regions, which indicates that marine heatwaves may have more increases of heatwave frequency and duration than those in the land (Fig. 2c,d).

Some regions will experience longer and more frequent heatwaves. The increases of heatwave frequency and duration are much greater in South America (SA), southern and central Africa (SCAF) than the other selected domains (Fig. 2c,d). One of the reasons is that tropical regions tend to have the largest changes in heatwave frequency and duration (Fig. S1e,g) and the two domains (SA and SCAF) have more tropical grid cells. However, contributions from land-atmosphere interactions to the increases of heatwave frequency and duration are not as significant in South America and SCAF as those in the other five domains.

Land-atmosphere interactions constitute a significant component in the projected change of all the four heatwave characteristics. Compared with heatwave mean intensity, land-atmosphere interactions tend to make more contributions to the total change of the other three heatwave characteristics. Among the seven land domains, land-atmosphere interactions tend to have the least significant effects on the projected

changes of all the four heatwave characteristics in southern and central Africa. In addition, excluding South America and SCAF, land-atmosphere interactions are found to be especially strong in East, North, and central Asia (ENCA), Australia (AU), the US, West Europe (WE), and East Europe and West Asia (EEWA) in the perspectives of the three heatwave characteristics (HWAt, HWF, and HWD). These domains are the so-called heatwave hotspots where the land-atmosphere interactions are more important in amplifying heatwave conditions than in other domains.

Contributions from land-atmosphere interactions to the four heatwave characteristics are different, land-atmosphere interactions are stronger in controlling the increases of heatwave mean intensity (about 0.4 °C) in Australia and South America (Fig. 2a). By contrast, more percentages taken up by land-atmosphere interactions in the total change in heatwave peak intensity compared with mean intensity indicates that the role of land-atmosphere interactions is more significant in inducing more increases for the intensity of the hottest heatwaves than for mean heatwave intensity. Compared with southern and central Africa (an increase below 0.2 °C), soil moisture has a greater effect in increasing the temperature of the hottest heatwave (HWAt) by 0.3–1 °C in other selected domains (Fig. 2b). Compared with South America and SCAF (about 1%), contributions of land-atmosphere interactions to heatwave frequency are greater in ENCA, Australia, the US, West Europe, and EEWA, as they induce an increase of 2–5% in heatwave frequency for these domains (Fig. 2c). Land-atmosphere interactions contribute to an extension of 10 days in heatwave duration for the US and about 5–10 days for the other domains (Fig. 2d).

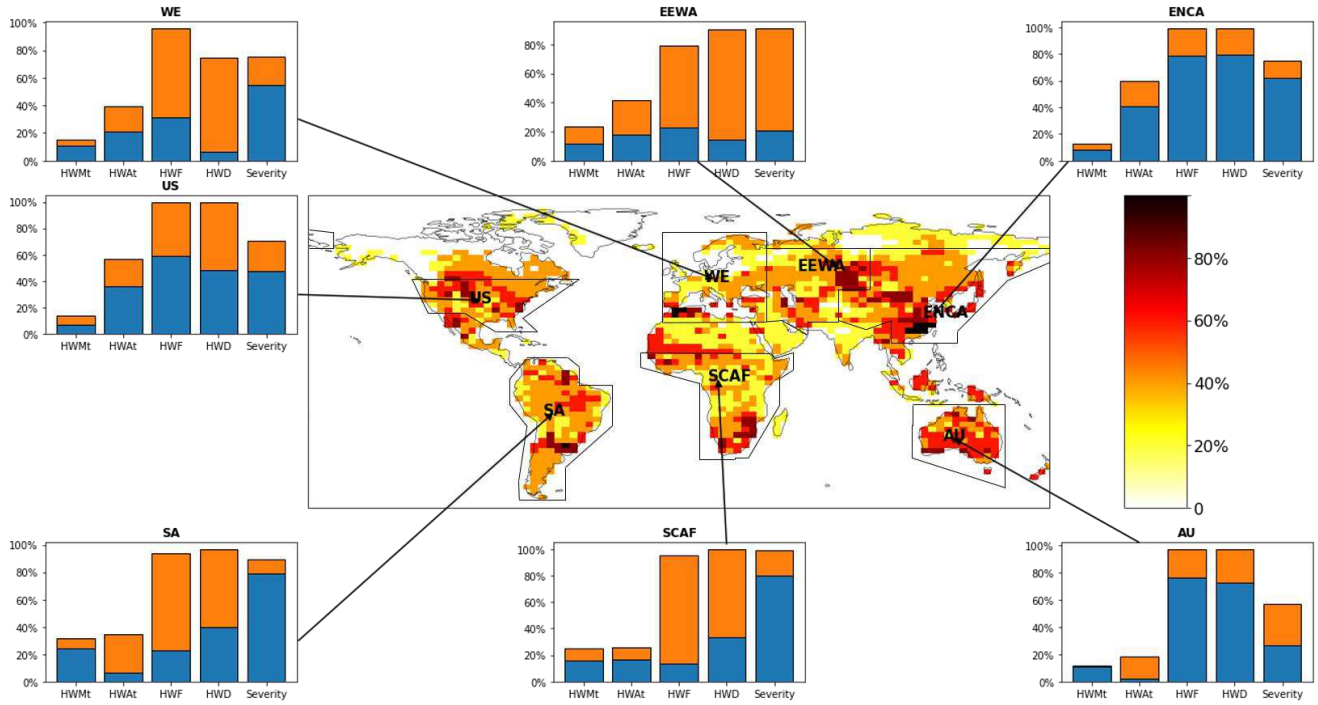

Fig. 3 | Projected change of population exposure to heatwaves. Increases of heatwaves' impacts on the human population induced by land-atmosphere interactions and other factors are shown in the form of five different heatwave characteristics, which includes heatwave mean intensity (HWMt), peak intensity (HWAt), frequency (HWF), duration (HWD), and severity. The change is between 2070–2100 and 1980–2010 and is calculated between the population percentage that is above the threshold (HWMt, 20.5 °C; HWAt, 32 °C; HWF, 3%; HWD, 5 days; Severity, 1) in both present period (1980–2010) and future period (2070–2100). The population data is of 2020. The map indicates the synthetical increases of the population exposure based on five heatwave characteristics. In the barplots, the orange part indicates contributions from land-atmosphere interactions; the blue part indicates other factors such as cloud cover, radiation, and precipitation.

The change of population exposure to heatwaves, and the role of land-atmosphere interactions in defining that exposure are also investigated in this study. Population percentage that is above the threshold (HWMt, 20.5 °C; HWAt, 32 °C; HWF, 3%; HWD, 5 days; Severity, 1) in both present period (1980–2010) and future period (2070–2100) are compared to calculate the change of the population exposure. It is found that large increases in population exposure by the end of the century, which commonly reaches 50% of the local population count, are distributed widely across the world. Southern parts of ENCA, eastern and southeastern parts of EEWA, northern and southern parts of SCAF, northern and middle parts of South America, North and Southeast of the US, and most parts of Australia will experience a great increase (more than 60%) in population exposure to heatwave impacts (Fig. 3). By contrast, a different

phenomenon was found in European region (West Europe and western parts of EEWA) where most of the parts in this region will experience less increases (basically less than 40%) in population exposure to heatwave impacts (Fig. 3). One of the reasons is that most of the population in European region has already been exposed to heatwave impacts under the thresholds set in this study and the future increases in population exposure to heatwave impacts are not evident. Nevertheless, in European region, the increases in population exposure to heatwave impacts still cannot be discounted (normally above 20%). In all the selected domains (ENCA, EEWA, West Europe, South America, the US, Australia, and SCAF) except Australia, increases in population exposure to heatwave frequency, duration, and severity are the greatest (which are normally more than 60%) among all the five heatwave characteristics (Fig. 3). For heatwave mean intensity and peak intensity, the increases of population exposure to both heatwave characteristics are similar and also less (less than 40%) compared to the other three heatwave characteristics in South America, SCAF, and Australia (Fig. 3). In West Europe, EEWA, ENCA, and US, more increases of human exposure to heatwave peak intensity are found compared with those to heatwave mean intensity (Fig. 3).

Land-atmosphere interactions tend to make less contributions to increases of population exposure to heatwaves in both ENCA and Australia (Fig. 3). By contrast, in EEWA, land-atmosphere interactions contribute a significant component to the increases of population exposure to heatwaves in the perspectives of all the five heatwave characteristics (Fig. 3). Moreover, in all the selected domains, increases in population exposure to heatwave mean intensity are less compared to the other four heatwave characteristics, land-atmosphere interactions are also found to make less contributions to increases of population exposure to heatwave mean intensity (Fig. 3).

Conclusions

Heatwaves are projected to increase in their frequency, duration, mean intensity, and peak intensity for most mid-latitude land regions by the end of the 21st century (Fig. 3 and Fig. S1). This is consistent with many former studies[2,3,39,40]. Stronger relationship of extreme quantiles of both heatwave duration and frequency with soil moisture deficit was found over southeastern Europe versus central Europe[41]. In addition, the observational datasets utilized by Mueller et al. (2012) has a wider cover and it was showed that a strong land-atmosphere coupling exists in many areas of the world, including most areas of North and South America, Europe, Australia, and parts of East Asia[42].The areas in our study that were identified with strong land-atmosphere interactions (Fig. S2) tend to agree with observationally derived estimates[41,42]. Some former modelling studies have also indicated regional differences in soil moisture-temperature effects[28,43]. Study of Seneviratne et al. (2006) indicated a strong land-atmosphere interaction in central and eastern Europe[28]. Knist et al. (2017) also evaluated land-atmosphere coupling in the EURO-CORDEX simulations and found strong land-atmosphere interactions over southern Europe compared with the northern Europe[43]. It is consistent with our findings (Fig. S2) and the patterns in which land-atmosphere interactions are stronger in the southern parts of Europe, also applies to all other continents such as Asia, North America, South America, and Africa. The regions with the largest response of heatwave characteristics to land-atmosphere interactions are majorly distributed in mid-latitude areas in both hemispheres, which coincides with those identified with strong land-atmosphere interactions[19]. In addition, the influences of land-atmosphere interactions are found to be enhanced and expanding over most land regions (Fig. 1). The findings are consistent with the results of previous research on land surface contribution to heatwaves[20,44]. Lorenz et al. (2016) found that the influence of soil moisture is larger in the future, which is evident in the perspective of heatwave frequency[20].

The increasing land-atmosphere interactions constitute a significant component in the exacerbation of heatwaves especially in East, North, West, and central Asia (ENCA), Australia (AU), the US, Europe and West Asia (WE and EEWA) (Fig. 2). It confirms the results of some existing research that removing soil moisture variability will significantly weaken the temperature extremes over most land surfaces[20,40], it also partly confirms the results of Vogel et al. (2017) that projected changes of regional temperature due to land-atmosphere interactions in Central North America and Central Europe tend to be greater than those in Amazonia, southern Africa, and northern Australia[40]. In general, land-atmosphere interactions are more important for the increases of heatwave duration and frequency compared with those of the mean heatwave intensity (HWMt) and the intensity of the hottest heatwaves (HWAt) in the global land regions and in the perspectives of the five domains excluding South America and SCAF (Fig. 2), while the research conducted by Donat et al. (2017) indicated similar results that daily hot temperatures increase faster than the mean ones across GLACE-CMIP5[45]. Additionally, both Fischer et al. (2007) and Lorenz et al. (2010) show that land-atmosphere interactions are important for the persistence of heatwave days, which is also found in our results for heatwave duration (Fig. 2)[8,46]. However, the effects of land-atmosphere interactions on the change of population exposure are different compared to their effects on heatwave characteristics in each selected domain (Fig. 3).

Southern and eastern parts of ENCA, most parts of Australia, eastern parts of EEWA, northern parts of US, and southern parts of SCAF, are regions where most of the population will be exposed to heatwave impacts in the future (Fig. 3). Large increases in population exposure to heatwaves are found over densely populated regions such as eastern parts of US, southern parts of ENCA. Selected domains (ENCA, Australia, SCAF, South America, US, West Europe, and EEWA) are considered hotspots where land-atmosphere interactions and increases of population exposure to heatwaves are both significant. These

domains, some of which contain several subregions, need to be investigated in the future research regarding the risk of their populations under exacerbating heatwaves which are largely influenced by land-atmosphere interactions. In South America and SCAF, although land-atmosphere interactions are not strong enough to make a dominant component in contributing to increases of heatwave characteristics, they make significant impacts on increasing population exposure to heatwaves. Moreover, increasing population exposure to heatwave frequency, duration, and severity, are strong, which indicates that for considering policies addressing heatwave impacts on humans different heatwave characteristics can be incorporated in heatwave evaluation and more emphases should be put on these three heatwave characteristics in the future.

Future investigations on influences from background climate conditions are needed. Background climate may dominate changes of regional temperature compared to land use change or other land-atmosphere interactions, and is likely one of the reasons for contributions from land-atmosphere interactions to projected increases of heat extremes are less obvious in southern and central Africa (Fig. 2) [47-49]. Furthermore, occurrence and severity of heatwaves and their future changes under multiple compounding drivers deserve more research in the future. In addition to land-atmosphere interactions, heatwave evolution and variability are also related to natural climate variability. These potential drivers will evolve over time and alter the risk of future heatwaves. Taking climate indices as covariates or using sensitivity experiments based on model simulations can shed light on the effects of changes in natural variability and the corresponding impacts on occurrence and severity of future heatwaves.

In addition, as population exposure depends on both population attributes and heatwave characteristics, the trend of future population needs to be considered as well in the future research to constrain uncertainties in simulating changes of population exposure to heatwaves. For subregions such as Arctic

regions in Russia, Far East in Russia, Tibetan Plateau, the impacts of heatwaves measured through increases of population exposure are mild from a population perspective as these regions have low population count. However, the exacerbation of heatwave conditions to these regions will still cause catastrophic impacts on the local ecosystems as the ecosystems in these regions are fragile and extremely vulnerable to climate change. Moreover, populations are not equally exposed to heatwaves, for example, population in some regions may have access to advanced cooling systems or well-insulated buildings while the others may not. In this way, the situations where the population are will be incorporated in the future research to improve the evaluation of population exposure to heatwaves.

The same heatwave temperature threshold (T_{90}) throughout the present period of 1980–2010 and future period of 2070–2100 contributes partly to the situation where all the selected heatwave characteristics, except for heatwave severity, increased significantly (Figs. 2 and S1). Changes in both spatial and temporal dimensions of heatwaves strongly depend on the selected threshold as strong increases in heatwave characteristics are detected if time-invariant climatic thresholds are adopted while minor changes are found in these characteristics when moving thresholds are defined[50]. Even though time-invariant climatic thresholds have been utilized to investigate land contributions to temperature extremes in numerous former studies[46,51,52], moving thresholds may be more widely utilized in the future studies.

More future studies on regional differences of heatwave impacts, which may integrate finer spatial resolutions of climate model results and recent historical simulations on spatial distributions of land-atmosphere interactions, heatwave characteristics, and human populations, are needed to better find local thresholds of heatwave characteristics and account for the local changes of human exposure to heatwaves. In addition, as large differences exist between climate models, which is related to complicated combinations of atmospheric forcing (precipitation), energy partitioning (sensible and latent heating) at

the surface, and how the soil moisture is represented[20,44], different climate models show a significant spread when representing different climatic variables. This is a common problem with CMIP5 and also CMIP6 outputs[53], so the research is focused on the ensemble mean. Future research will incorporate effects of individual climate models on the ensemble mean to improve simulation results of the model ensemble.

Methods

Heatwave identification and classification

Heatwaves can be characterized in different ways[52,54]. We use a modified excess heat factor (EHF) to define such events where at least three consecutive days are above a threshold temperature [3,55]. Numerous national meteorological agencies such as the Australian Bureau of Meteorology, Met Office in UK, and National Oceanic and Atmospheric Administration (NOAA) have used or are considering using the excess heat factor (EHF) to identify heatwave days and describe important characteristics of heatwaves[56,57]. A modified version of EHF is used in this study to identify heatwave days[54,58]. This index can be expressed as:

$$EHF_{sig} = T_{3d} - T_{90} = \frac{(T_t + T_{t+1} + T_{t+2})}{3} - T_{90} \quad (1)$$

where T_t is the average daily temperature for day t, and T_{90} is the calendar day 90th percentile of daily average temperature using all the reference years investigated (1950–2014). The average daily temperature is defined as the average of T_{min} (i.e., daily minimum temperature) and T_{max} (i.e., daily maximum temperature) within a 24-hour cycle. T_{90} is estimated using a 15-day window (i.e., 7 days before and after the calendar day with a temperature T_t) for all reference years to provide a sample of 975 (15 x 65) daily values per grid cell. Positive values of EHF_{sig} define heatwave-like conditions for day *t*. If the T_{3d} is above the threshold of T_{90} for at least three consecutive days (i.e., *t*, *t*+1, and *t*+2), these days are regarded as heatwave days.

Once the heatwave days have been identified, different heatwave characteristics can be determined. In this study, different characteristics of heatwave such as duration of the seasonal longest heatwave (HWD); average magnitude for all seasonal heatwaves (HWMt); temperature at the peak of the heatwave with the hottest average (HWAt); number of heatwave days (HWF), which is expressed as the percentage relative to the total number of days, are analyzed.

Moreover, although EHF_{sig} is used in most analyses in this study, to account for acclimatization relevant for human health applications, EHF_{accl} is defined as the three-day-averaged daily mean temperature compared against the average daily mean temperature over the recent past, while EHF_{sig} is with respect to the long-term climate. EHF_{accl} is described as:

$$EHF_{accl} = \frac{(T_1 + T_{t+1} + T_{t+2})}{3} - \frac{(T_{t+1} + \cdots + T_{t+30})}{30} \quad (2)$$

Both EHF_{sig} and EHF_{accl} can be thought of as sustained temperature anomalies and can be combined to derive:

$$EHF = \max(1, EHF_{accl}) \times EHF_{sig} \quad (3)$$

A product of EHF_{accl} and EHF_{sig} will be used to calculate the *EHF* when trying to calculate the different heatwave characteristics (HWAt, HWMt, HWD, HWF, and severity) in evaluating population exposure to heatwaves. The threshold for heatwave severity is obtained by computing the 85th percentile (EHF_{85}) of all the positive *EHF* values within the climatology period 1950–2014. The ratios of *EHF* and EHF_{85} are used to indicate the heatwave severity, which can be classified to different levels[58].

The heatwaves during the summer-centering period are the focus of our research. The summer-centering period in the Northern Hemisphere is defined as May, Jun., Jul., Aug., and Sep.; the summer-centering period in the Southern Hemisphere is defined as Nov., Dec., Jan., Feb., and Mar. Moreover, Jan., Feb., and Mar. of the next year are moved forward to the year before to calculate summer heatwave characteristics of a specific year in the Southern Hemisphere.

Measurement of land-atmosphere interactions

The GLACE—CMIP5 experiment[19] has previously been used to investigate the role of land-atmosphere interactions[19,20,40,44]. The results of CTL minus ExpA are used to indicate land-atmosphere interactions. Statistical significance in comparisons between land-atmosphere interactions in present period (1980–2010) and future period (2070–2100) is assessed using a two-tailed Mann-Whitney U test[59] because the results in present period and future period are both 30 years and the two sample of ranks are independent. This nonparametric test is used to determine whether the results in both periods are distinguishable at a 99% confidence level[3]. To determine the total contributions of land-atmosphere interactions to the changes in temperature extremes at regional scales, projected changes in heatwave peak intensity, mean intensity, duration, frequency, and severity are computed, the differences of the changes between CTL and ExpA express the contributions of land-atmosphere interactions to changes in heatwave characteristics.

GlACE-CMIP5

Table 1| Earth System Models Participating in GLACE-CMIP5 (for more details, see Seneviratne et al. (2013))[19]

Acronym	Atmospheric Model	Land Surface Model	Resolution (lon. × lat.)	References
ACCESS	Atmospheric Unified Model 7.3 (UM)	Community Atmosphere Biosphere Land Exchange (CABLE) Land Surface Model 2.0	1.875° × 1.25°	Davies et al. (2005)[60], Martin et al. (2006)[61], Wang and Leuning (1998)[62], and Lorenz et al. (2014)[63]
CESM	National Center for Atmospheric Research Community Atmospheric Model (CAM4)	Community Land Model (CLM4)	1.25° × 0.942°	Neale et al. (2013)[64] and Lawrence et al. (2011)[65]
EC–EARTH	Integrated Forecasting System European Centre for Medium-range Weather Forecasts (IFS)	Hydrology-Tiled ECMWF Scheme for Surface Exchange over Land (H-TESSEL)	1.125° × 1.121°	Hazeleger et al. (2011)[66] and Balsamo et al. (2009)[67]
GFDL	Geophysical Fluid Dynamics Laboratory Earth System Model 2 (ESM2)	Land Model 3.0 (LM3.0)	2.5° × 2.011°	Dunne et al. (2012)[68] and Shevliakova et al. (2009)[69]
IPSL	Laboratoire de Météorologie Dynamique Atmospheric Model (LMDZ5A)	Organizing Carbon and Hydrology in Dynamic Ecosystems (ORCHIDEE) with Two-Layer Hydrology Scheme	3.75° × 1.895°	Dufresne et al. (2013)[70], Hourdin et al. (2012)[71], and Cheruy et al. (2012) [72]
MPI-ESM	European Centre/Hamburg Forecast System	Jena Scheme for Biosphere–Atmosphere Coupling in Hamburg (JSBACH)	1.875° × 1.865°	Stevens et al. (2013)[73], Hagemann, Loew, and Andersson (2013)[74], Raddatz et al. (2007)[75], and Brovkin et al. (2009)[76]

GLACE—CMIP5 were often used in previous research to investigate the role of land-atmosphere interactions[20,40,44]. GLACE—CMIP5 consists of six state-of-the art climate models (Table 1) in which the control run (CTL) and experiment A (ExpA) have been used to effectively measure land-atmosphere interactions in the form of CTL−ExpA[19,20,44]. The control run is a fully coupled simulation. For ExpA, soil moisture is prescribed by the past (1971–2000) climatological values calculated from the control simulation.

For consistency, climate model datasets will be interpolated into a common grid of 3.75° longitude by 2.5° latitude using a conservative remapping approach[37,38]. The interpolation will make it feasible to use ensemble mean of climate models in this research.

Population dataset and exposure

Gridded data of global population count for the year 2020, were used in this project to investigate population exposure to heatwaves[36]. While some population data in different years are available, it is more appropriate to consider the change in exposure in the context of today's population. The population datasets, which were adjusted to match United Nations country

totals, were consistent with national censuses and population registers in respect to relative spatial distributions. The spatial resolution of this dataset was 1˚ longitude by 1˚ latitude. Population count was taken into account to assess population exposure to different heatwave characteristics in the scale of subregions.

For consistency, population data was interpolated into a common grid of 3.75° longitude by 2.5° latitude using a conservative remapping approach[37,38]. The interpolation enabled quantifications of population exposure to heatwaves, which was calculated as the following:

$$\Delta PE = (P_{fut} - P_{pre})/P_{all} \quad (4)$$

In a certain region, ΔPE indicates the change of population exposure, P_{fut} indicates the future population count above a certain threshold of one heatwave characteristic, P_{pre} indicates the current population count above a certain threshold of the heatwave characteristic, P_{all} is whole population count.

Data Availability

The GLACE-CMIP5 data is available from Sonia I. Seneviratne at ETH Zurich (sonia.seneviratne@ethz.ch). Gridded data of global population count is available from Socioeconomic Data and Applications Center of National Aeronautics and Space Administration (NASA), https://sedac.ciesin.columbia.edu/data/collection/gpw-v4.

Acknowledgements

The authors acknowledge the modelling contributors of the GLACE-CMIP5 experiment for access to the modelling data.

Author Contributions

J.Z performed the analysis with extensive help from A.L.H., S.I.S. provided GLACE-CMIP5 data. J.Z interpreted the results with the input from A.J.T. and A.L.H., J.Z. wrote the paper with useful comments from A.L.H., A.J.T., and S.I.S. All authors reviewed and edited the manuscript before submission.

Competing Interests

The authors declare no competing interests.

References

1 Ding, T. & Qian, W. Geographical patterns and temporal variations of regional dry and wet heatwave events in China during 1960–2008. *Advances in Atmospheric Sciences* **28**, 322-337, doi:10.1007/s00376-010-9236-7 (2011).

2 Perkins, S. E., Alexander, L. V. & Nairn, J. R. Increasing frequency, intensity and duration of observed global heatwaves and warm spells. *Geophysical Research Letters* **39**, doi:10.1029/2012gl053361 (2012).

3 Cowan, T. *et al.* More Frequent, Longer, and Hotter Heat Waves for Australia in the Twenty-First Century. *Journal of Climate* **27**, 5851-5871, doi:10.1175/jcli-d-14-00092.1 (2014).

4 Miralles, D. G., Teuling, A. J., van Heerwaarden, C. C. & Vilà-Guerau de Arellano, J. Mega-heatwave temperatures due to combined soil desiccation and atmospheric heat accumulation. *Nature Geoscience* **7**, 345-349, doi:10.1038/ngeo2141 (2014).

5 Perkins-Kirkpatrick, S. E. & Lewis, S. C. Increasing trends in regional heatwaves. *Nat Commun* **11**, 3357, doi:10.1038/s41467-020-16970-7 (2020).

6 Seneviratne, S. I. *et al.* in *Climate Change 2021: The Physical Science Basis. Contribution of Working Group I to the Sixth Assessment Report of the Intergovernmental Panel on Climate Change* (eds V. Masson-Delmotte *et al.*) 1513–1766 (Cambridge University Press, 2021).

7 Fischer, E. M., Seneviratne, S. I., Vidale, P. L., Lüthi, D. & Schär, C. Soil Moisture–Atmosphere Interactions during the 2003 European Summer Heat Wave. *Journal of Climate* **20**, 5081-5099, doi:10.1175/jcli4288.1 (2007).

8 Fischer, E. M., Seneviratne, S. I., Lüthi, D. & Schär, C. Contribution of land-atmosphere coupling to recent European summer heat waves. *Geophysical Research Letters* **34**, doi:10.1029/2006gl029068 (2007).

9 Teuling, A. J. & Seneviratne, S. I. Contrasting spectral changes limit albedo impact on land-atmosphere coupling during the 2003 European heat wave. *Geophysical Research Letters* **35**, doi:10.1029/2007gl032778 (2008).

10 Otto, F. E. L., Massey, N., van Oldenborgh, G. J., Jones, R. G. & Allen, M. R. Reconciling two approaches to attribution of the 2010 Russian heat wave. *Geophysical Research Letters* **39**, n/a-n/a, doi:10.1029/2011gl050422 (2012).

11 Trenberth, K. E. & Fasullo, J. T. Climate extremes and climate change: The Russian heat wave and other climate extremes of 2010. *Journal of Geophysical Research: Atmospheres* **117**, n/a-n/a, doi:10.1029/2012jd018020 (2012).

12 *State of the Climate: Global Climate Report for August 2020*, <https://www.ncdc.noaa.gov/sotc/global/202008> (2020).

13 Lewis, S. C. & Karoly, D. J. Anthropogenic contributions to Australia's record summer temperatures of 2013. *Geophysical Research Letters* **40**, 3705-3709, doi:10.1002/grl.50673 (2013).

14 Lewis, S. C. & King, A. D. Dramatically increased rate of observed hot record breaking in recent Australian temperatures. *Geophysical Research Letters* **42**, 7776-7784, doi:10.1002/2015gl065793 (2015).

15 Hirsch, A. L. *et al. Amplification of Australian heatwaves via local land-atmosphere*

coupling (2019).

16 *State of the Climate: Global Climate Report for Annual 2020*, <https://www.ncdc.noaa.gov/sotc/global/202013> (2020).

17 Seneviratne, S. I. *et al.* Investigating soil moisture–climate interactions in a changing climate: A review. *Earth-Science Reviews* **99**, 125-161, doi:10.1016/j.earscirev.2010.02.004 (2010).

18 Zhang, J., Wu, L. & Dong, W. Land-atmosphere coupling and summer climate variability over East Asia. *Journal of Geophysical Research* **116**, doi:10.1029/2010jd014714 (2011).

19 Seneviratne, S. I. *et al.* Impact of soil moisture-climate feedbacks on CMIP5 projections: First results from the GLACE-CMIP5 experiment. *Geophysical Research Letters* **40**, 5212-5217, doi:10.1002/grl.50956 (2013).

20 Lorenz, R. *et al.* Influence of land-atmosphere feedbacks on temperature and precipitation extremes in the GLACE-CMIP5 ensemble. *Journal of Geophysical Research: Atmospheres* **121**, 607-623, doi:10.1002/2015jd024053 (2016).

21 Hauser, M., Orth, R. & Seneviratne, S. I. Role of soil moisture versus recent climate change for the 2010 heat wave in western Russia. *Geophysical Research Letters* **43**, 2819-2826, doi:10.1002/2016gl068036 (2016).

22 Vogel, M. M., Zscheischler, J. & Seneviratne, S. I. Varying soil moisture–atmosphere feedbacks explain divergent temperature extremes and precipitation projections in central Europe. *Earth System Dynamics* **9**, 1107-1125, doi:10.5194/esd-9-1107-2018 (2018).

23 Teuling, A. J. *et al.* Contrasting response of European forest and grassland energy exchange to heatwaves. *Nature Geoscience* **3**, 722-727, doi:10.1038/ngeo950 (2010).

24 Russo, S., Sillmann, J. & Fischer, E. M. Top ten European heatwaves since 1950 and their occurrence in the coming decades. *Environmental Research Letters* **10**, doi:10.1088/1748-9326/10/12/124003 (2015).

25 Ding, T., Qian, W. & Yan, Z. Changes in hot days and heat waves in China during 1961-2007. *International Journal of Climatology*, n/a-n/a, doi:10.1002/joc.1989 (2009).

26 Grotjahn, R. *et al.* North American extreme temperature events and related large scale meteorological patterns: a review of statistical methods, dynamics, modeling, and trends. *Climate Dynamics* **46**, 1151-1184, doi:10.1007/s00382-015-2638-6 (2015).

27 Miralles, D. G., Gentine, P., Seneviratne, S. I. & Teuling, A. J. Land-atmospheric feedbacks during droughts and heatwaves: state of the science and current challenges. *Ann N Y Acad Sci* **1436**, 19-35, doi:10.1111/nyas.13912 (2019).

28 Seneviratne, S. I., Luthi, D., Litschi, M. & Schar, C. Land-atmosphere coupling and climate change in Europe. *Nature* **443**, 205-209, doi:10.1038/nature05095 (2006).

29 Jones, B., Tebaldi, C., O'Neill, B. C., Oleson, K. W. & Gao, J. Avoiding population exposure to heat-related extremes: demographic change vs climate change. *Climatic Change* **146**, 423-437, doi:10.1007/s10584-017-2133-7 (2018).

30 Margolis, H. G. in *Global Climate Change and Public Health* Ch. Chapter 6, 85-120 (2014).

31 Gasparrini, A. *et al.* Mortality risk attributable to high and low ambient temperature: a multicountry observational study. *The Lancet* **386**, 369-375, doi:10.1016/s0140-6736(14)62114-0 (2015).

32 Vicedo-Cabrera, A. M. *et al.* The burden of heat-related mortality attributable to recent human-induced climate change. *Nature Climate Change* **11**, 492-500,

doi:10.1038/s41558-021-01058-x (2021).

33 Mishra, V., Mukherjee, S., Kumar, R. & Stone, D. A. Heat wave exposure in India in current, 1.5 °C, and 2.0 °C worlds. *Environmental Research Letters* **12**, doi:10.1088/1748-9326/aa9388 (2017).

34 Yang, J. *et al.* Projecting heat-related excess mortality under climate change scenarios in China. *Nat Commun* **12**, 1039, doi:10.1038/s41467-021-21305-1 (2021).

35 Xu, Z., FitzGerald, G., Guo, Y., Jalaludin, B. & Tong, S. Impact of heatwave on mortality under different heatwave definitions: A systematic review and meta-analysis. *Environ Int* **89-90**, 193-203, doi:10.1016/j.envint.2016.02.007 (2016).

36 CIESIN. Gridded Population of the World, Version 4 (GPWv4): Population Density Adjusted to Match 2015 Revision UN WPP Country Totals, Revision 11. (2018).

37 Hanke, M., Redler, R., Holfeld, T. & Yastremsky, M. YAC 1.2.0: new aspects for coupling software in Earth system modelling. *Geoscientific Model Development* **9**, 2755-2769, doi:10.5194/gmd-9-2755-2016 (2016).

38 Hanke, M. & Redler, R. New features with YAC 1.5.0. *Reports on ICON*, doi:10.5676/DWD (2019).

39 Russo, S. *et al.* Magnitude of extreme heat waves in present climate and their projection in a warming world. *Journal of Geophysical Research: Atmospheres* **119**, 12,500-512,512, doi:10.1002/2014jd022098 (2014).

40 Vogel, M. M. *et al.* Regional amplification of projected changes in extreme temperatures strongly controlled by soil moisture-temperature feedbacks. *Geophysical Research Letters* **44**, 1511-1519, doi:10.1002/2016gl071235 (2017).

41 Hirschi, M. *et al.* Observational evidence for soil-moisture impact on hot extremes in southeastern Europe. *Nature Geoscience* **4**, 17-21, doi:10.1038/ngeo1032 (2010).

42 Mueller, B. & Seneviratne, S. I. Hot days induced by precipitation deficits at the global scale. *Proc Natl Acad Sci U S A* **109**, 12398-12403, doi:10.1073/pnas.1204330109 (2012).

43 Knist, S. *et al.* Land-atmosphere coupling in EURO-CORDEX evaluation experiments. *Journal of Geophysical Research: Atmospheres* **122**, 79-103, doi:10.1002/2016jd025476 (2017).

44 Lorenz, R., Pitman, A. J., Hirsch, A. L. & Srbinovsky, J. Intraseasonal versus Interannual Measures of Land–Atmosphere Coupling Strength in a Global Climate Model: GLACE-1 versus GLACE-CMIP5 Experiments in ACCESS1.3b. *Journal of Hydrometeorology* **16**, 2276-2295, doi:10.1175/jhm-d-14-0206.1 (2015).

45 Donat, M. G., Pitman, A. J. & Seneviratne, S. I. Regional warming of hot extremes accelerated by surface energy fluxes. *Geophysical Research Letters* **44**, 7011-7019, doi:10.1002/2017gl073733 (2017).

46 Lorenz, R., Jaeger, E. B. & Seneviratne, S. I. Persistence of heat waves and its link to soil moisture memory. *Geophysical Research Letters* **37**, n/a-n/a, doi:10.1029/2010gl042764 (2010).

47 Li, Y. *et al.* The role of spatial scale and background climate in the latitudinal temperature response to deforestation. *Earth System Dynamics* **7**, 167-181, doi:10.5194/esd-7-167-2016 (2016).

48 Zhao, L., Lee, X., Smith, R. B. & Oleson, K. Strong contributions of local background climate to urban heat islands. *Nature* **511**, 216-219, doi:10.1038/nature13462 (2014).

49 Pitman, A. J. *et al.* Importance of background climate in determining impact of land-cover change on regional climate. *Nature Climate Change* **1**, 472-475, doi:10.1038/nclimate1294 (2011).

50 Vogel, M. M., Zscheischler, J., Fischer, E. M. & Seneviratne, S. I. Development of Future Heatwaves for Different Hazard Thresholds. *Journal of Geophysical Research: Atmospheres* **125**, doi:10.1029/2019jd032070 (2020).

51 Coumou, D. & Robinson, A. Historic and future increase in the global land area affected by monthly heat extremes. *Environmental Research Letters* **8**, doi:10.1088/1748-9326/8/3/034018 (2013).

52 Perkins, S. E. A review on the scientific understanding of heatwaves—Their measurement, driving mechanisms, and changes at the global scale. *Atmospheric Research* **164-165**, 242-267, doi:10.1016/j.atmosres.2015.05.014 (2015).

53 Hirsch, A. L., Ridder, N. N., Perkins-Kirkpatrick, S. E. & Ukkola, A. CMIP6 Multi-Model Evaluation of Present - Day Heatwave Attributes. *Geophysical Research Letters*, doi:10.1029/2021gl095161 (2021).

54 Perkins, S. E. & Alexander, L. V. On the Measurement of Heat Waves. *Journal of Climate* **26**, 4500-4517, doi:10.1175/jcli-d-12-00383.1 (2013).

55 Perkins, S. E., Argüeso, D. & White, C. J. Relationships between climate variability, soil moisture, and Australian heatwaves. *Journal of Geophysical Research: Atmospheres* **120**, 8144-8164, doi:10.1002/2015jd023592 (2015).

56 Nairn, J., Ostendorf, B. & Bi, P. Performance of Excess Heat Factor Severity as a Global Heatwave Health Impact Index. *Int J Environ Res Public Health* **15**, doi:10.3390/ijerph15112494 (2018).

57 Hudson, D. & Marshall, A. G. Extending the Bureau's heatwave forecast to multi-week timescales. (Bureau of Meteorology, 2016).

58 Nairn, J. R. & Fawcett, R. J. The excess heat factor: a metric for heatwave intensity and its use in classifying heatwave severity. *Int J Environ Res Public Health* **12**, 227-253, doi:10.3390/ijerph120100227 (2014).

59 Mann, H. B. & Whitney, D. R. On a Test of Whether one of Two Random Variables is Stochastically Larger than the Other. *The Annals of Mathematical Statistics* **18**, 50-60 (1947).

60 Davies, T. *et al.* A new dynamical core for the Met Office's global and regional modelling of the atmosphere. *Quarterly Journal of the Royal Meteorological Society* **131**, 1759-1782, doi:10.1256/qj.04.101 (2005).

61 Martin, G. M. *et al.* The Physical Properties of the Atmosphere in the New Hadley Centre Global Environmental Model (HadGEM1). Part I: Model Description and Global Climatology. *Journal of Climate* **19**, 1274–1301, doi:10.1175/JCLI3636.1 (2006).

62 Wang, Y. P. & Leuning, R. A two-leaf model for canopy conductance, photosynthesis and partitioning of available energy I:: Model description and comparison with a multi-layered model. *Agricultural and Forest Meteorology* **91**, 89-111, doi:10.1016/S0168-1923(98)00061-6 (1998).

63 Lorenz, R. *et al.* Representation of climate extreme indices in the ACCESS1.3b coupled atmosphere–land surface model. *Geoscientific Model Development* **7**, 545-567, doi:10.5194/gmd-7-545-2014 (2014).

64 Neale, R. B. *et al.* The Mean Climate of the Community Atmosphere Model (CAM4) in Forced SST and Fully Coupled Experiments. *Journal of Climate* **26**, 5150-5168, doi:10.1175/jcli-d-12-00236.1 (2013).

65 Lawrence, D. M. *et al.* Parameterization improvements and functional and structural advances in Version 4 of the Community Land Model. *Journal of Advances in Modeling Earth Systems* **3**, doi:10.1029/2011ms000045 (2011).

66 Hazeleger, W. *et al.* EC-Earth V2.2: description and validation of a new seamless earth system prediction model. *Climate Dynamics* **39**, 2611-2629, doi:10.1007/s00382-011-1228-5 (2011).

67 Balsamo, G. *et al.* A Revised Hydrology for the ECMWF Model: Verification from Field Site to Terrestrial Water Storage and Impact in the Integrated Forecast System. *Journal of Hydrometeorology* **10**, 623-643, doi:10.1175/2008jhm1068.1 (2009).

68 Dunne, J. P. *et al.* GFDL's ESM2 Global Coupled Climate–Carbon Earth System Models. Part I: Physical Formulation and Baseline Simulation Characteristics. *Journal of Climate* **25**, 6646-6665, doi:10.1175/jcli-d-11-00560.1 (2012).

69 Shevliakova, E. *et al.* Carbon cycling under 300 years of land use change: Importance of the secondary vegetation sink. *Global Biogeochemical Cycles* **23**, n/a-n/a, doi:10.1029/2007gb003176 (2009).

70 Dufresne, J. L. *et al.* Climate change projections using the IPSL-CM5 Earth System Model: from CMIP3 to CMIP5. *Climate Dynamics* **40**, 2123-2165, doi:10.1007/s00382-012-1636-1 (2013).

71 Hourdin, F. *et al.* Impact of the LMDZ atmospheric grid configuration on the climate and sensitivity of the IPSL-CM5A coupled model. *Climate Dynamics* **40**, 2167-2192, doi:10.1007/s00382-012-1411-3 (2012).

72 Cheruy, F. *et al.* Combined influence of atmospheric physics and soil hydrology on the simulated meteorology at the SIRTA atmospheric observatory. *Climate Dynamics* **40**, 2251-2269, doi:10.1007/s00382-012-1469-y (2012).

73 Stevens, B. *et al.* Atmospheric component of the MPI-M Earth System Model: ECHAM6. *Journal of Advances in Modeling Earth Systems* **5**, 146-172, doi:10.1002/jame.20015 (2013).

74 Hagemann, S., Loew, A. & Andersson, A. Combined evaluation of MPI-ESM land surface water and energy fluxes. *Journal of Advances in Modeling Earth Systems*, n/a-n/a, doi:10.1029/2012ms000173 (2013).

75 Raddatz, T. J. *et al.* Will the tropical land biosphere dominate the climate–carbon cycle feedback during the twenty-first century? *Climate Dynamics* **29**, 565-574, doi:10.1007/s00382-007-0247-8 (2007).

76 Brovkin, V., Raddatz, T. J., Reick, C. H., Claussen, M. & Gayler, V. Global biogeophysical interactions between forest and climate. *Geophysical Research Letters* **36**, n/a-n/a, doi:10.1029/2009gl037543 (2009).

Supplementary Files

This is a list of supplementary files associated with this preprint. Click to download.

- SupplementaryMaterial.pdf